ACS OMEGA

http://pubs.acs.org/journal/acsodf

Article

Optimization of Chitosan-Decorated Solid Lipid Nanoparticles for Improved Flurbiprofen Transdermal Delivery

Firdous Ahmad Burki, Kifayat Ullah Shah,* Ghulam Razaque, Shefaat Ullah Shah, Asif Nawaz, Muhammad Danish Saeed, Maqsood Ur Rehman, Hadia Bibi, Mulham Alfatama, and Tarek M. Elsayed

Cite This: *ACS Omega* 2023, 8, 19302−19310

Read Online

ACCESS | Metrics & More | Article Recommendations

ABSTRACT: Transdermal delivery is a potential alternative route to oral administration for drugs associated with stomach discomfort, such as flurbiprofen, a widely nonsteroidal anti-inflammatory drug (NSAID). This study aimed to design solid lipid nanoparticle (SLN) transdermal formulations of flurbiprofen. Chitosan-coated SLNs were prepared by the solvent emulsification method, and their properties and permeation profiles across the excised rat skin were characterized. The particle size of uncoated SLNs was at 695 ± 4.65 nm, which increased to 714 ± 6.13, 847 ± 5.38, and 900 ± 8.65 nm upon coating with 0.05, 0.10, and 0.20% of chitosan, respectively. The drug association efficiency was improved when a higher concentration of chitosan was employed over SLN droplets that endowed a higher affinity of flurbiprofen with chitosan. The drug release was significantly retarded as compared to the uncoated entities and followed non-Fickian anomalous diffusion that was depicted by "*n*" values of >0.5 and <1. Also, the total permeation of chitosan-coated SLNs (F7−F9) was significantly higher than that of the noncoated formulation (F5). Overall, this study has successfully designed a suitable carrier system of chitosan-coated SLNs that provide insight into the current conventional therapeutic approaches and suggest new directions for the advancements in transdermal drug delivery systems for improved permeation of flurbiprofen.

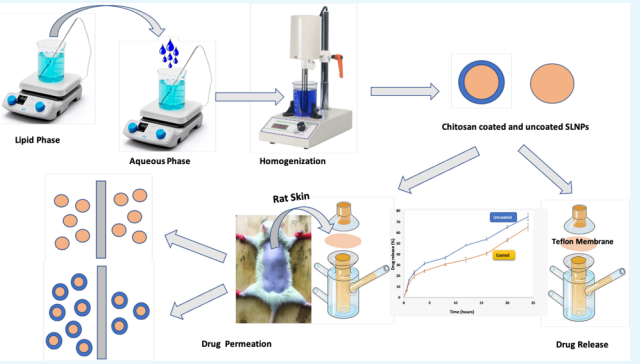

1. INTRODUCTION

Conventional dermal formulations possess various limitations that include but are not limited to loss of dosage due to atmospheric deterioration, limited bioavailability (1.0−15%), and variation of release characteristics of the dried residue from the originally applied ones.[1] These formulations exhibit poor penetration abilities through the dead keratinized stratum corneum layer of the skin.[2] On the other hand, oral therapeutic administration can be a challenge for the disabled or elderly, young children, or unattainable for unconscious patients in a coma, while intravenous drug delivery carries the risk of infections and necessitates qualified people.[3]

The alternative noninvasive approaches to transdermal drug delivery systems are envisaged as promising approaches to enhance and control drug transport across the skin, thus overcoming the aforementioned previous limitations while improving the safety and efficacy of marketed drugs.[4] The practical advantages of transdermal drug delivery are the avoidance of a chemically hostile environment of the gastrointestinal tract, first-pass metabolism in the liver, and drug-associated limitations like a narrow therapeutic index and short biological half-life.[5] In this approach, active ingredients are applied to the skin in the form of spray, gel, or patches and transported in a noninvasive manner that enables less risk of overdose, stable blood levels, greater stability of the active ingredient, and prolonged therapeutic effect.[6] Therefore, attempts to transform existing drugs into user-friendly transdermal dosage forms have been widely taking place to improve adherence and tolerance, reduce dosing frequency, obtain sustained drug release, use in a diverse population, and minimize central nervous system adverse effects.[7] These advantages of transdermal drug delivery compel pharmaceutical scientists to take a keen interest in the skin as the site of drug delivery for both local and systemic effects.

SLNs, as an alternative to conventional carriers, such as liposomes and nanoemulsions, were initially introduced as drug carriers in 1991.[8] Superiorly to the ordinary carriers, SLNs possess advantages, including sustained drug release, high physical stability, and the capability of scaling up with

Received: December 22, 2022
Accepted: May 8, 2023
Published: May 21, 2023

negated use of organic solvents.[9] SLNs are basically synthesized from a solid lipid core and a monolayer of surfactant shell. Bioactive compounds, especially lipophilic molecules, can be embedded into the solid lipid matrix.[10] Among nanocarriers, SLNs are highly promising drug delivery systems applied for effective protection and controlled release of bioactive molecules from external conditions while exhibiting excellent biodegradability and low toxicity.[11] These carriers are mainly prepared from physiological lipids dispersed in an aqueous solution and aided with a surfactant.[12] The preparation process of SLNs is simple, with the ability to be conducted under sterile conditions and the capability to incorporate both hydrophilic and lipophilic drugs.[13] The SLNs exhibit high stability and can be effectively utilized in controlling and site-specific drug-targeting delivery due to their small size and relatively narrow size distribution.[14] Since these nanovectors are made of physiological lipids, their acute and chronic toxicities are minimized.[15] SLNs enable utmost control over the release profile and protect sensitive lipophilic drugs from environmental degradation compared to liquid lipid carriers.[16] The physicochemical properties of SLNs exhibit a fundamental role in transdermal drug delivery, where the binding function is mainly governed by particle charge, whereas internalization is mediated by the size and shape of entities. Other features like viscosity, density, and surface tensions can also influence attachment, internalization, and retention of drugs in the skin.[17]

Biopolymer coating and surface modification of SLNs have been used to improve interactions between the cells and SLNs that mediate cellular uptake and enhance the SLNs' delivery efficiency.[18] Pharmaceutically, the natural polymer chitosan has shown an increasing interest in different formulations.[19] It is a natural polysaccharide derived from chitin by means of partial deacetylation. Chitosan is extensively utilized in various fields, including food, cosmetics, and agricultural industries, owing to its excellent biodegradability, biocompatibility, and toxicological safety.[20] Recently, chitosan has emerged as a coating material in the area of pharmaceutical nanotechnology for many carriers, such as metal nanoparticles, polymeric nanoparticles, and SLNs.[21−23] Reports have attributed the physicochemical property alteration of these nanoparticles to the positive charge endowed by chitosan to the nanocarrier surfaces.[24] Elaborating cell interactions and tissue penetration, extending drug release, improving physicochemical stability, and improving bioavailability and drug efficacy were found after nanoparticle chitosan coating.[25−27]

Flurbiprofen is a potent anti-inflammatory drug that possesses poor skin permeability, while the oral dosage forms are associated with adverse effects like gastrointestinal ulceration, constipation, and bleeding. It has a short half-life of 3.9 h, requiring frequent oral dosing. The pharmacokinetic analysis has shown that topically applied flurbiprofen can achieve higher drug concentration within the target tissues (tendon, muscle, periosteal, and fat tissues) with respect to orally administered flurbiprofen administered under the regulatory approved dosing guidelines.[28] Therefore, the current study attempts to prepare chitosan-coated SLNs to improve the skin permeability of flurbiprofen by means of permeation enhancer properties of chitosan, small particle size, and lipoidal nature of SLNs.

2. MATERIALS AND METHODS

2.1. Chemicals. Flurbiprofen was supplied by Fozan Pharmaceuticals (Peshawar, Pakistan). Stearic acid (Sigma-Aldrich) was used as a solid lipid. Tween 80 (Sigma-Aldrich) was used as an emulsifier, and ethanol (Sigma-Aldrich) was used as a cosurfactant. Low-molecular-weight (50000 daltons) chitosan (Sigma-Aldrich) was used as the coating material.

2.2. Animals. In this study, all animal experiments complied with the guide of the National Institutes of Health for the laboratory use and care of animals (NIH publications No. 8023, revised 1978). The approval of the experimental protocol was given by Institutional Animal Ethics Committee, Gomal University (approval no. 204/QEC/GU dated 18/05/2020). Thirty healthy male Albino Wister rats at the age of 14 weeks (weighing 250 ± 30 g) were purchased from the animal house, Gomal University, housed in plastic cages at room temperature with 12 h light/dark cycle, fed with standard chew diet and water ad libitum, and kept in isolation for 7 days.

2.3. Preparation of Solid Lipid Nanoparticles. The SLN was prepared by the solvent emulsification evaporation method as described previously.[29] The formulation was first optimized using different amounts of surfactant (Tween 80) and cosurfactant (ethanol). The optimized clear homogeneous preparation was then coated with different concentrations of chitosan (Table 1). Briefly, 1.0 g of stearic acid was melted in a water bath at 70 °C. Flurbiprofen (0.05 g) was then added with continuous magnetic stirring at the same temperature. Later, ethanol (20 g) was then added to get the lipid phase. The aqueous phase was prepared by adding 1.5 g of Tween 80 to distilled water and stirring continuously for 1 h at 70 °C. The lipid phase was added dropwise to an aqueous phase with continuous magnetic stirring to obtain the final formulation. The complete removal of ethanol with continuous magnetic stirring at 70 °C has negated the possible aggregation. The resultant colloidal dispersion was homogenized using a homogenizer (Ultra-Turrax, T45, DX, Japan).

Table 1. Composition of Tested SLN Formulations[a]

formulation	drug (g)	stearic acid (g)	tween 80 (g)	ethanol (g)	chitosan (g)	distilled water (g)
F1	0.05	1.00	1.00	15.00	0.00	82.95
F2	0.05	1.00	1.50	15.00	0.00	82.45
F3	0.05	1.00	2.00	15.00	0.00	81.95
F4	0.05	1.00	1.50	15.00	0.00	82.45
F5	0.05	1.00	1.50	20.00	0.00	77.45
F6	0.05	1.00	1.50	25.00	0.00	72.45
F7	0.05	1.00	1.50	20.00	0.05	72.40
F8	0.05	1.00	1.50	20.00	0.10	72.30
F9	0.05	1.00	1.50	20.00	0.20	72.10

[a]Note: F5 was optimized formulation, which was then coated with chitosan (F7−F9).

2.4. Characterization of the Prepared SLNs. The selected SLN formulations (F5 and F7−F9) were characterized for their size, size distribution, charge, pH, density, surface tension, viscosity, morphology, drug content, entrapment efficiency, and drug release behavior.

2.4.1. ζ Potential. The zeta potential of the SLN droplets was determined using a Zetasizer Nano ZS90 (Malvern Instruments; Worcestershire, U.K.) at 25 ± 1 °C using a sample quantity of 700 μL loaded in the folded capillary cell integrated with a gold electrode. Three measurements were

https://doi.org/10.1021/acsomega.2c08135
ACS Omega 2023, 8, 19302−19310

conducted, and the results are shown as mean ± standard deviation.

2.4.2. pH. The pH of the prepared SLNs was evaluated using a pH meter (Accumet meter 21039, Denver Instruments) at 25 ± 1 °C after calibration of the instrument with known buffer solutions of pH 3, 7, and 9. The readings are shown as mean ± standard deviation of triplicate results.

2.4.3. Density/Specific Gravity. The density of the SLNs was calculated using a common laboratory pycnometer at 25 ± 1 °C. The weight of a known volume of an empty pycnometer, the weight of the pycnometer with water, and the weight of the pycnometer with SLNs were determined using an electronic balance (AX120, SHIMADZU, Japan). The density and specific gravity of SLN formulations were then calculated using eqs 1−3, respectively

$$\text{density of water} = W_2/V \tag{1}$$

$$\text{density of SLNs} = W_3/V \tag{2}$$

$$\text{specific gravity of SLNs} = \text{density of SLNs}/\text{density of water} \tag{3}$$

where V is the volume of the pycnometer, W_1 is the weight of the empty pycnometer, W_2 is the weight of the water-filled pycnometer, and W_3 is the weight of the SLN-filled pycnometer.

2.4.4. Surface Tension. The surface tension of the formulations was determined using a commonly used laboratory stalagmometer (Louisiana). The distilled water was filled up to mark A and then allowed to flow drop-by-drop up to mark B. The number of drops was calculated and taken as mean ± SD of triplicate results. The same procedure was repeated for the SLN formulations. Density was calculated as mentioned earlier in Section 2.4.3 The surface tension was calculated using eq 4 at 25 ± 1 °C.

$$\gamma_1 = (\delta_1 \times n_1 \div \delta_2 \times n_2) \times \gamma_2 \tag{4}$$

where γ_1 is the surface tension of the SLN sample; γ_2 is the surface tension of deionized water, i.e., 72.8 dynes/cm; δ_1 is the density of the SLN sample; δ_2 is the density of distilled water; n_1 is the number of drops of the SLN sample; and n_2 is the number of drops of distilled water.

2.4.5. Viscosity. The viscosity of the formulations was calculated using an Ostwald viscometer provided with capillary tube type B (Poulten Selfe & Lee Ltd., Essex, U.K.). The viscometer was washed, cleaned, and dried. The apparatus was fixed on a vertical stand. Distilled water was filled up to mark A and allowed to flow from point A to B, and the time was recorded. The same procedure was repeated for SLN formulations. The viscosity of the prepared SLNs was calculated using eq 5.[30] All readings were taken as mean ± SD at 25 ± 1 °C of triplicate results.

$$\eta_1 = (t_1 \times d_1 - t_2 \times d_2) \times \eta_2 \tag{5}$$

where η_1 is the viscosity of the provided SLN sample, η_2 is the viscosity of deionized water, t_1 is the time of flow of the SLN sample, t_2 is the time of flow of deionized water, d_1 is the density of the SLN sample, and d_2 is the density of deionized water.

2.4.6. Morphology. The detailed structure of both uncoated and coated SLNs was observed using a scanning electron microscope (SEM, JSM 910, JEOL Japan). The SLNs were centrifuged at 12000 rpm for 5 min to remove the aqueous phase from the dispersed SLNs. Osmium tetroxide (3 drops) was added to the sediment as a fixation medium and was kept at 8 °C for 2 h. The sample was diluted with 0.1 M phosphate buffer as a washing medium. The process of washing and centrifugation was repeated twice. The samples were then dehydrated using acetone. Then, an aliquot of SLNs was put on the carbon film using a 400 mesh copper grid for analysis. The selected areas were photographed at an accelerating voltage of 20 kV and a magnification level of 20000×.

2.4.7. Drug Content and Entrapment Efficiency. The drug content and entrapment efficiency were determined using a UV spectrophotometer. Exactly 1 gram of SLNs was taken in an Eppendorf tube (Cat no 007103; SCILOGEX) and centrifuged (D3024, SCILOGEX) at 13 000 rpm for 15 min. The supernatant (0.5 mL) was suitably diluted with phosphate buffer pH 7.4. The sample was then stirred for 10 min at 1000 rpm with a magnetic stirrer. The absorbance was recorded at λ_{max} of 248 nm[31] using a UV spectrophotometer (UV-1601, SHIMADZU, Japan).

The sediment was mixed with 1 mL of methanol and vortexed for 5 min to extract the entrapped drug from the SLNs. It was diluted with phosphate buffer (pH 7.4) and further stirred for 10 min. The absorbance was recorded at λ_{max} of 248 nm using a UV−visible spectrophotometer. The drug content which is the quotient of drug concentration with respect to the total amount of drug-loaded SLNs is calculated as the sum of the drug in both supernatant and sediment.[32] The drug entrapment and association efficiencies were calculated using eqs 6 and 7, respectively.[33]

$$\text{drug entrapment efficiency} = [(\text{added drug} - \text{free drug})/(\text{drug added})] \times 100 \tag{6}$$

$$\text{drug association efficiency} = [(\text{free drug} + \text{entrapped drug})/(\text{total drug})] \times 100 \tag{7}$$

2.4.8. FTIR Analysis. The FTIR analysis of drug, chitosan, and SLNs was carried out using attenuated total reflectance-Fourier transform infrared spectroscopy (ATR-FTIR, L1600300 spectrum TWO LITA, Llantrisant, U.K.). Briefly, 3 mg of the liquid SLN drops was put on a germanium diamond disc. The sample was scanned over a wavelength range of 400−4000 cm^{-1}. The force gauge of 40 N was applied in the case of solid samples. The characteristic peaks of IR transmission spectra were recorded in triplicate.

2.4.9. Drug Release. The release profile of both coated and uncoated SLNs was determined using a Teflon membrane (Chromacol) having a pore size of 0.45 μm as partitioning media between the donor and recipient compartments of Franz diffusion cell (Perme Gear, Inc., No: 4G-01-00-15-12, India; diffusion area = 1.767 cm^2). The receptor compartment was filled with 5.0 ml of freshly prepared phosphate buffer pH 5.5 as simulated skin fluid with a temperature of 32 ± 2 °C. The samples (1 mL) were taken at different time intervals from the receptor compartment and similarly replaced using the same amount of phosphate buffer. These samples were analyzed using a UV spectrophotometer (UV-1601 SHIMADZU, Japan). All of the results were recorded as mean ± SD of triplicate analysis. The mechanism of drug release was described by fitting the release data into the power law kinetic model and expressed in eq 8[34]

https://doi.org/10.1021/acsomega.2c08135
ACS Omega 2023, 8, 19302−19310

$$M_t/M_\infty = K t^n \quad (8)$$

where M_t and M_∞ show the fraction of drug released after time t; K is the release rate constant; and n represents the exponential value of the release exponent that determines the release mechanism, where n = <0.543 depicts the quasi-Fickian diffusion mechanism, n = 0.43 depicts the Fickian diffusion mechanism, n = 0.43 to < 0.585 depicts the drug release mechanism of anomalous, non-Fickian transport for spherical systems, n = 85 depicts case II transport or zero-order release mechanism, while n = 0 to > 85 shows the zero-order release mechanism or super case II transport.

2.4.10. Drug Permeation Study. The rats were sacrificed by cervical dislocation, and the abdominal skin was shaved to remove the hairs. The skin was then surgically isolated from the abdominal area, and subcutaneous fat was removed. The skin (thickness = 0.80 ± 0.09 mm) was measured by a digital Vernier caliper (MITUTOYO, Japan), washed with 0.9% w/v sodium chloride physiological solution, wrapped in an aluminum foil, and stored for further study.

The skin was clamped between the donor and recipient compartments of Franz diffusion cell (Perme Gear, Inc. No:4G-01-00-15-12) in such a manner that the epidermis faces the formulation and dermis layer toward the receptor compartment. The phosphate buffer pH 7.4 was filled into the recipient compartment having 7 mL capacity to provide sink condition. The diffusion cells were maintained at 37 ± 2 °C using a recirculating water bath. The quantity of formulation containing exactly 491 μg of flurbiprofen was applied to the skin on the donor compartment. The aliquots (1 mL) of the fluid in the receptor chambers were withdrawn for analysis at different time intervals, which were then similarly replaced with fresh solvent. The samples were analyzed using a UV−visible spectrophotometer, and the results are shown as mean ± SD. The cumulative amounts of flurbiprofen permeated through rat skins were plotted as a function of time.

2.5. Statistical Analysis. All analyses were carried out in triplicate, and the results are shown as mean ± standard deviation. The data were analyzed using SPSS software version 18 (SPSS Inc., Chicago). ANOVA and/or Student's *t*-test with $p < 0.05$ indicates a statistically significant difference denoted by $p < 0.05$.

3. RESULTS AND DISCUSSION

3.1. Preparation of SLNs. The SLNs were prepared using stearic acid as the physiological lipid that is widely available, is relatively cheap, and dissolves soluble flurbiprofen.[35] Tween 80 was added as an emulsifier due to its HLB value, surface tension-reducing properties, stearic ability, nonionic nature, and improved permeation enhancement attribute.[36] The particle size determined using photon correlation spectroscopy for the optimized SLN formulation (F5) was larger as compared to their SEM results (Table 2 and Figure 1). The particle size of coated formulations increases with the increasing concentration of chitosan in formulation.[37] Though particles of approximately 600 nm are required for optimum transdermal drug delivery,[38] the results have shown that lipoidal particles of 695−900 nm (that were actually smaller as per scanning electron microscopy findings) can optimally penetrate through the skin layers due to the synergistic permeation enhancer effect of Tween 80 and chitosan along with increased absorption properties of solid lipids (Table 2 and Figure 3). Since the chitosan-decorated particles were mostly heterogeneous, as depicted by their polydispersity index values of greater than 0.5 (Table 2), smaller particles could have been responsible for improved permeation.

Table 2. Size, Polydispersity Index, and ζ Potential of the SLNs

formulation	size (nm)	PDI	charge (mV)
F5	695 ± 4.65	0.125	−30.00
F7	714 ± 6.13	1.000	0.0032
F8	847 ± 5.38	1.000	0.3800
F9	900 ± 8.65	1.000	

3.2. Physicochemical Evaluation of the Prepared SLNs. The uncoated SLNs with a zeta potential of −30 mV were found to be stable due to the prevention of aggregation and Ostwald ripening by a mechanism of repulsive forces between similarly charged particles.[39] In the case of chitosan-coated formulations, the zeta potential turned positive due to free amino groups of chitosan, which is further expected to increase drug permeation mediated by electrostatic interaction with the negatively charged biological membranes.[40]

The physiological pH of the skin ranges from 4.9 to 5.9, while any disturbance due to applied formulations can favor bacterial growth (specifically staphylococcus aureus), resulting in inflammation, irritation, and enzymatic disturbances.[41] The pH of prepared SLNs was in the range of 4−6, being accepted for the application as a transdermal system (Table 3).

The surface tension is the force at the interface between two immiscible layers. The skin possesses surface tension of 27−28 dynes/cm that allows molecules of similar or fewer values of surface tension to adhere to the skin surface. SLNs are capable of reducing the interfacial tension between the skin and the loaded drug, thereby improving permeation across the stratum corneum.[42] These formulations spread easily on the skin surface and provide an increased surface area for permeation. The surface tension of the pharmaceutical formulation can also give a good prediction of drug release from the product.[43] The higher values of prepared SLNs' surface tension were attributed to the increased chain length of carbons in stearic acid, which is agreeable with previous reports (Table 3).[44,45]

The density affects the dynamic properties of the formulation and is a quotient of the weight-to-volume ratio. The density values of all optimized formulations were close to the unity of the density of deionized water (1 gm/cm^3). This is due to the fact that deionized water has been used as an aqueous phase forming the bulk of formulations. The higher density of chitosan-coated formulations (F7−F9) could be regarded as an increased mass median volume diameter and hence an enlarged surface area as compared to the formulation's weight (Table 3). The viscosity of the SLNs has been shown to be the product of an oily component, surfactants, and aqueous phase concentrations, and all parameters contribute to deciding the final consistency of prepared SLNs. The chitosan-coated formulations were more viscous as compared to coating-free SLNs, and water has a viscosity of 1.004 m^2/s × 10^{-6}. Formulations of higher viscosity could improve the retention of drugs in the stratum corneum layer of the skin (Table 3).

An optimized lipid concentration is required for the optimum entrapment of the drug.[29] Keeping in view the solubility of flurbiprofen in stearic acid, the drug content was found to be in the range of 0.40 to 0.49 mg/mL, whereby more than 80.0% of the drug was entrapped in the coated and

https://doi.org/10.1021/acsomega.2c08135
ACS Omega 2023, 8, 19302−19310

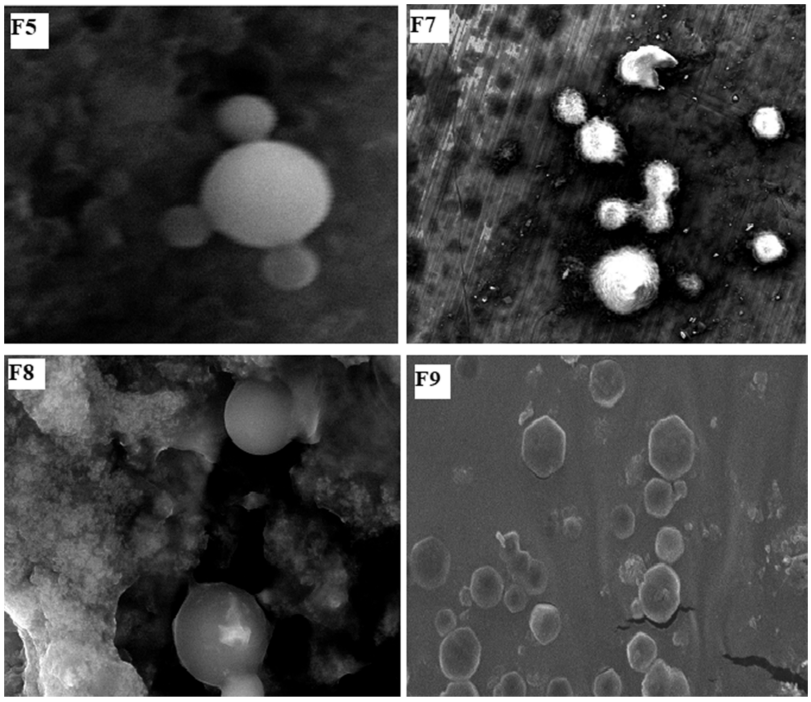

Figure 1. Scanning electron microscopy images of SLNs (F5) and SLN-coated chitosan (F7, F8, F9).

Table 3. Physicochemical Characteristics of Flurbiprofen-Loaded SLNs

code	pH	surface tension (dynes/cm^2)	density (kg/m^3)	viscosity (m^2/s)	drug content (mg/mL)	entrapment efficiency (%)	association efficiency (%)
F5	4.45 ± 0.9	77.24 ± 0.3	0.84 ± 0.2	1.45 ± 0.4	0.49 ± 0.2	75.96 ± 0.3	97.95
F7	4.20 ± 0.8	79.31 ± 0.5	0.96 ± 0.1	1.54 ± 0.3	0.49 ± 0.1	81.30 ± 0.1	96.11
F8	5.90 ± 0.5	88.66 ± 0.3	0.98 ± 0.3	1.55 ± 0.3	0.48 ± 0.1	82.17 ± 0.2	94.65
F9	6.10 ± 0.8	93.14 ± 0.5	0.99 ± 0.1	1.71 ± 0.2	0.40 ± 0.3	83.01 ± 0.3	80.26

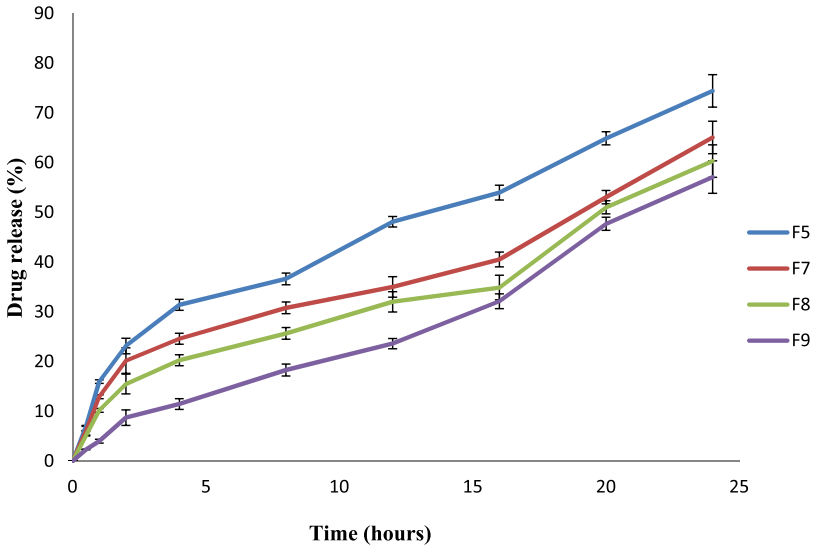

Figure 2. Cumulative percentage drug release from manufactured SLNs.

uncoated SLNs. The entrapped drug was expected to provide a slow release of the drug from prepared SLNs. Drug lipid affinity affects drug entrapment and association efficiency; hence, an improved drug entrapment could be attributed to the affinity of stearic acid and flurbiprofen, as shown in Table 3.[46]

3.3. Drug Release and Release Kinetics. The release of drugs from chitosan-coated SLNs was significantly retarded as compared to uncoated ones (Figure 2; ANOVA: $p < 0.05$). This could be explained by the decreased solubility of chitosan at physiological pH. The increased particle size of the chitosan-coated formulation can also contribute to controlling drug release from coated formulations (F7−F9). The drug entrapment efficiency of chitosan-coated formulations was higher and prolonged drug release from the coated SLNs. The drug

https://doi.org/10.1021/acsomega.2c08135
ACS Omega 2023, 8, 19302−19310

release patterns from the SLNs were determined using the power law kinetic model. The *n* value indicates the exponent of fractional drug release. When the *n* value is greater than 0.5 and less than 0.89, it indicates anomalous non-Fickian diffusion.[47] The *n* values of F5 to F8 were >0.5 and less than 1, which depicts the non-Fickian anomalous diffusion mechanism of drug release, whereas the *n* value of F9 was at 0.917 that approached nearly ideal zero-order kinetics, depicting that the release from SLNs is primarily associated with controlled swelling of chitosan (Table 4).[48]

Table 4. Kinetic Models and Mechanism of Drug Release from Both Coated and Uncoated SLNs

	power law kinetic model			
formulations	$K \pm$ SD	R^2	*n*	release Mechanism
F5	0.053 ± 0.1664	0.9192	0.609	anomalous non-Fickian diffusion
F7	0.018 ± 0.3153	0.9178	0.616	anomalous non-Fickian diffusion
F8	0.217 ± 0.5604	0.9465	0.665	anomalous non-Fickian diffusion
F9	3.436 ± 8.144	0.9776	0.917	anomalous non-Fickian diffusion

3.4. Ex Vivo Permeation Study. The permeation of chitosan-coated SLNs (F7−F9) was significantly higher than that of the noncoated formulation (F5) (Figure 3; ANOVA: $p < 0.05$). The flux rate for 24 h permeation study was found to be at 29.46, 41.00, 33.04, and 33.43 (percent/cm^2·h) for F5, F7, F8, and F9, respectively. The increased permeation was attributed to the interaction of the positively charged chitosan with the negatively charged lipid and protein domains of the skin stratum corneum.[49] The above interaction may cause disorganization of skin lipids and alter secondary structures, thereby resulting in larger pores and increased permeation by intercellular and/or transcellular route. On the other hand, Tween 80 enabled lipid packing fluidization, skin lipid extraction, and increased water content of the stratum corneum.[50] The summative effects reduce the barrier function of the epidermis, thereby facilitating transdermal drug transport. The negative charge of F5 could also be responsible for retarded drug permeation through the negatively charged skin surface. The abrupt increase in permeation after 16 h was due to supersaturation that induced skin penetration and permeation of lipophilic drugs like flurbiprofen.[51]

3.5. ATR-FTIR Analysis. The FTIR analysis of pure drug, polymer, and formulations was carried out to confirm the interactions of the drug with formulation excipients. The main peaks for pure drug (flurbiprofen) were observed at wavenumbers 1217, 1321, 2973, and 3670 cm^{-1} representing aromatic ring, C═C stretching, a carboxyl group (COOH), and asymmetric CH_2, respectively.[52] The peaks at wavenumbers 3363 and 2988 cm^{-1} were also observed in optimized formulations (Figure 4). The additional peaks that appeared at the wavenumber 1635 cm^{-1} in optimized formulations were ascribed to the presence of chitosan.[53] Incorporation of the drug into the SLNs had negated effects on their functional groups. This indicates that there is no interaction between the drug and polymer (chitosan) used in the present study.

The success of designed chitosan-coated SLNs has been elaborated from the chemical compatibility of formulation components based on FTIR analysis. The physicochemical properties of SLN, including pH, viscosity, and drug content, were found to be optimum for skin drug application. Similarly, the release and permeation analysis have shown preferential deposition in the skin for transdermal application.

4. CONCLUSIONS

The study has successfully synthesized flurbiprofen-loaded SLNs for transdermal drug delivery by the solvent emulsification method. Both chitosan-coated and uncoated SLNs achieved suitable physicochemical characteristics for administration through the skin. The in vitro release study depicted sustained release behavior due to the encapsulation of the drug within the solid lipid. The release was further retarded when chitosan was used as a coat over the negatively charged droplets of stearic acid. The uncoated SLNs bear a negative charge, whereas chitosan brought a positive charge on the surface of the nanoentities. The reduced viscosity and surface tension, along with the lipophilic nature of the drug-loaded SLNs, have resulted in enhanced permeation of the drug through the skin. The formulation components demonstrated the absence of interaction with the polymer and encapsulated

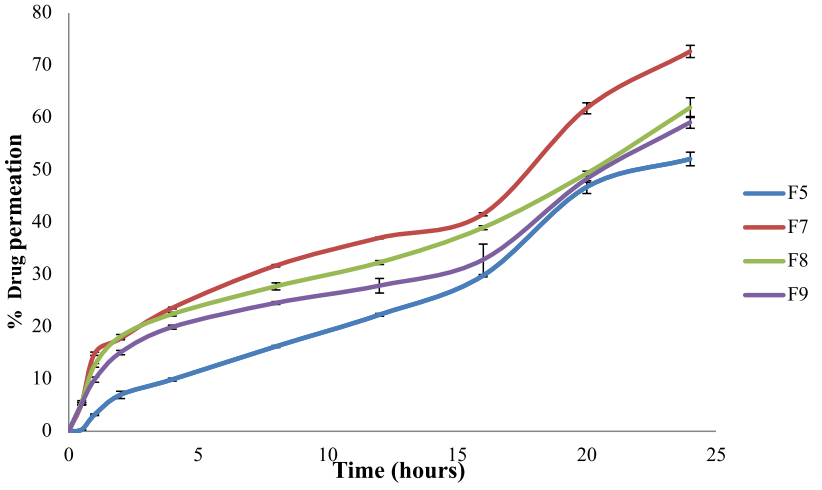

Figure 3. Cumulative permeation percentage of the drug through the skin.

https://doi.org/10.1021/acsomega.2c08135
ACS Omega 2023, 8, 19302−19310

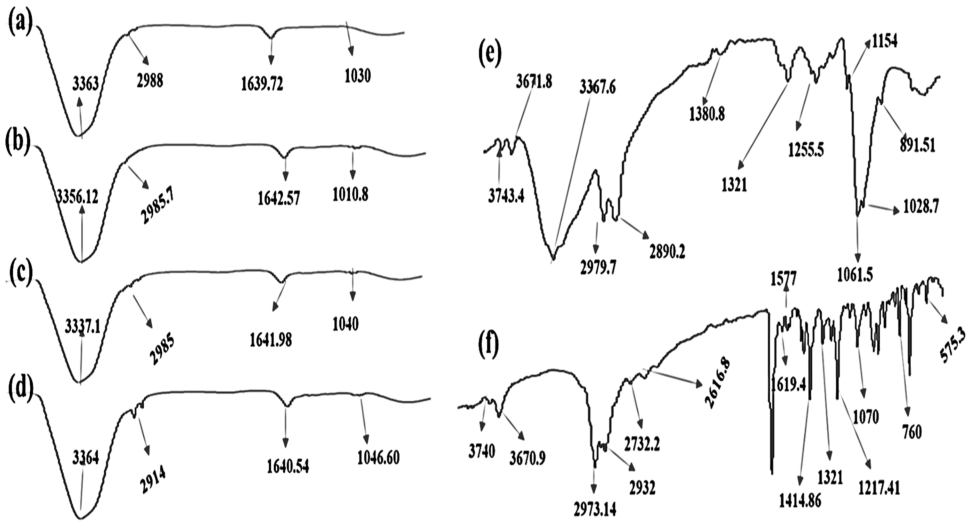

Figure 4. FTIR spectra of (a) F5, (b) F7, (c) F8, (d) F9, (e) chitosan, and (f) flurbiprofen.

drug, as confirmed by ATR/FTIR analysis. Overall, both chitosan-coated and uncoated formulations can achieve optimum drug permeation due to lipoidal interaction between solid lipid and phospholipid bilayers of the skin.

AUTHOR INFORMATION

Corresponding Author

Kifayat Ullah Shah − *Particle Design and Drug Deliveryery Laboratory, Faculty of Pharmacy, Gomal University, Dera Ismail Khan 29050 Khyber Pakhtunkhwa, Pakistan*; Email: kifayatrph@gmail.com

Authors

Firdous Ahmad Burki − *Particle Design and Drug Deliveryery Laboratory, Faculty of Pharmacy, Gomal University, Dera Ismail Khan 29050 Khyber Pakhtunkhwa, Pakistan*

Ghulam Razaque − *Faculty of Pharmacy and Health Sciences, University of Balochistan, Quetta 08770, Pakistan*

Shefaat Ullah Shah − *Particle Design and Drug Deliveryery Laboratory, Faculty of Pharmacy, Gomal University, Dera Ismail Khan 29050 Khyber Pakhtunkhwa, Pakistan*

Asif Nawaz − *Particle Design and Drug Deliveryery Laboratory, Faculty of Pharmacy, Gomal University, Dera Ismail Khan 29050 Khyber Pakhtunkhwa, Pakistan*

Muhammad Danish Saeed − *Particle Design and Drug Deliveryery Laboratory, Faculty of Pharmacy, Gomal University, Dera Ismail Khan 29050 Khyber Pakhtunkhwa, Pakistan*

Maqsood Ur Rehman − *Department of Pharmacy, Faculty of Sciences, University of Malakand, Dir Lower 18800 Khyber Pakhtunkhwa, Pakistan*

Hadia Bibi − *Department of Pharmacy, Women Institute of Learning, Abbottabad 22080 Khyber Pakhtunkhwa, Pakistan*

Mulham Alfatama − *Faculty of Pharmacy, Universiti Sultan Zainal Abidin, Besut Campus, Besut 22200, Malaysia*

Tarek M. Elsayed − *Faculty of Pharmacy, Universiti Sultan Zainal Abidin, Besut Campus, Besut 22200, Malaysia*; orcid.org/0000-0003-4592-7064

Complete contact information is available at: https://pubs.acs.org/10.1021/acsomega.2c08135

Author Contributions

F.A.B., A.N., K.A.K.: Conceptualization, methodology, writing—original draft. K.U..: Supervision. S.U.S., M.U.R., H.B.: Data curation and formal analysis. M.D.S., T.M.E., M.A.: Validation, resources, writing—review and editing.

Funding

This work was supported by the "Higher Education Commission of Pakistan" under an NRPU grant number 9226. The research was funded by Sultan Universiti Sultan Zainal Abidin (UniSZA) through UniSZA/2021/DPU2.0/05 grant (grant number R0332).

Notes

The authors declare no competing financial interest.

ACKNOWLEDGMENTS

The authors would like to thank Gomal University, Pakistan, and Universiti Sultan Zainal Abidin, Malaysia, for the technical and facilities support.

REFERENCES

(1) Bariya, S. H.; Gohel, M. C.; Mehta, T. A.; Sharma, O. P. Microneedles: An Emerging Transdermal Drug Deliveryery System. *J. Pharm. Pharmacol.* **2011**, *64*, 11−29.

(2) Garg, T.; Rath, G.; Goyal, A. K. Comprehensive Review on Additives of Topical Dosage Forms for Drug Deliveryery. *Drug Delivery* **2015**, *22*, 969−987.

(3) Radwan-Pragłowska, J.; Janus, Ł.; Piątkowski, M.; Sierakowska, A.; Matysek, D. ZnO Nanorods Functionalized with Chitosan Hydrogels Crosslinked with Azelaic Acid for Transdermal Drug Deliveryery. *Colloids Surf., B* **2020**, *194*, No. 111170.

(4) Chaturvedi, S.; Garg, A. An Insight of Techniques for the Assessment of Permeation Flux across the Skin for Optimization of Topical and Transdermal Drug Deliveryery Systems. *J. Drug Delivery Sci. Technol.* **2021**, *62*, No. 102355.

(5) Long, L.-y.; Zhang, J.; Yang, Z.; Guo, Y.; Hu, X.; Wang, Y. Transdermal Delivery of Peptide and Protein Drugs: Strategies, Advantages and Disadvantages. *J. Drug Delivery Sci. Technol.* **2020**, *60*, No. 102007.

(6) Jayaneththi, V. R.; Aw, K.; Sharma, M.; Wen, J.; Svirskis, D.; McDaid, A. J. Controlled Transdermal Drug Deliveryery Using a Wireless Magnetic Microneedle Patch: Preclinical Device Development. *Sens. Actuators, B* **2019**, *297*, No. 126708.

https://doi.org/10.1021/acsomega.2c08135
ACS Omega 2023, 8, 19302−19310

(7) Tijani, A. O.; Nunez, E.; Singh, K.; Khanna, G.; Puri, A. Transdermal Route: A Viable Option for Systemic Delivery of Antidepressants. *J. Pharm. Sci.* **2021**, *110*, 3129−3149.
(8) Müller, R. H.; Mehnert, W.; Lucks, J.-S.; Schwarz, C.; Mühlen, A. Z. Solid Lipid Nanoparticles (SLN): An Alternative Colloidal Carrier System for Controlled Drug Deliveryery. *Eur. J. Pharm. Biopharm.* **1995**, *41*, 62−69.
(9) Dawoud, M. Chitosan Coated Solid Lipid Nanoparticles as Promising Carriers for Docetaxel. *J. Drug Delivery Sci. Technol.* **2021**, *62*, No. 102409.
(10) Salah, E.; Abouelfetouh, M. M.; Pan, Y.; Chen, D.; Xie, S. Solid Lipid Nanoparticles for Enhanced Oral Absorption: A Review. *Colloids Surf., B* **2020**, *196*, No. 111305.
(11) Katopodi, A.; Anastasia, D. Solid Lipid Nanoparticles and Nanostructured Lipid Carriers of Natural Products as Promising Systems for Their Bioactivity Enhancement: The Case of Essential Oils and Flavonoids. *Colloids Surf., A* **2021**, *630*, No. 127529.
(12) Lippacher, A.; Müller, R. H.; Mäder, K. Liquid and Semisolid SLN Dispersions for Topical Application: Rheological Characterization. *Eur. J. Pharm. Biopharm.* **2004**, *58*, 561−567.
(13) Müller, R. H.; Mäder, K.; Gohla, S. Solid Lipid Nanoparticles (SLN) for Controlled Drug Deliveryery−a Review of the State of the Art. *Eur. J. Pharm. Biopharm.* **2000**, *50*, 161−177.
(14) Elzoghby, A. O.; Samy, W. M.; Elgindy, N. A. Albumin-Based Nanoparticles as Potential Controlled Release Drug Deliveryery Systems. *J. Controlled Release* **2012**, *157*, 168−182.
(15) Eniola-Adefeso, O.; Heslinga, M. J.; Porter, T. M. Design of Nano Vectors for Therapy and Imaging of Cardiovascular Diseases. *Methodist Debakey Cardiovasc. J.* **2021**, *8*, 13−17.
(16) Yadav, N.; Khatak, S.; Sara, U. V. S. Solid Lipid Nanoparticles-a Review. *Int. J. Appl. Pharm* **2013**, *5*, 8−18.
(17) Beddoes, C. M.; Case, C. P.; Briscoe, W. H. Understanding Nanoparticle Cellular Entry: A Physicochemical Perspective. *Adv. Colloid Interface Sci.* **2015**, *218*, 48−68.
(18) Yang, B.; Jiang, J.; Jiang, L.; Zheng, P.; Wang, F.; Zhou, Y.; Chen, Z.; Li, M.; Lian, M.; Tang, S.; et al. Chitosan Mediated Solid Lipid Nanoparticles for Enhanced Liver Delivery of Zedoary Turmeric Oil in Vivo. *Int. J. Biol. Macromol.* **2020**, *149*, 108−115.
(19) Mosavi, S. H.; Zare-Dorabei, R. Synthesis of NMOF-5 Using Microwave and Coating with Chitosan: A Smart Biocompatible PH-Responsive Nanocarrier for 6-Mercaptopurine Release on MCF-7 Cell Lines. *ACS Biomater. Sci. Eng.* **2022**, *8*, 2477−2488.
(20) Zhang, X.; Ismail, B. B.; Cheng, H.; Jin, T. Z.; Qian, M.; Arabi, S. A.; Liu, D.; Guo, M. Emerging Chitosan-Essential Oil Films and Coatings for Food Preservation-A Review of Advances and Applications. *Carbohydr. Polym.* **2021**, *273*, No. 118616.
(21) Ling Tan, J. S.; Roberts, C. J.; Billa, N. Mucoadhesive Chitosan-Coated Nanostructured Lipid Carriers for Oral Delivery of Amphotericin B. *Pharm. Dev. Technol.* **2019**, *24*, 504−512.
(22) Rabelo, R. S.; Oliveira, I. F.; da Silva, V. M.; Prata, A. S.; Hubinger, M. D. Chitosan Coated Nanostructured Lipid Carriers (NLCs) for Loading Vitamin D: A Physical Stability Study. *Int. J. Biol. Macromol.* **2018**, *119*, 902−912.
(23) Vieira, A. C. C.; Chaves, L. L.; Pinheiro, S.; Pinto, S.; Pinheiro, M.; Lima, S. C.; Ferreira, D.; Sarmento, B.; Reis, S. Mucoadhesive Chitosan-Coated Solid Lipid Nanoparticles for Better Management of Tuberculosis. *Int. J. Pharm.* **2018**, *536*, 478−485.
(24) Hosseini-Ashtiani, N.; Tadjarodi, A.; Zare-Dorabei, R. Low Molecular Weight Chitosan-Cyanocobalamin Nanoparticles for Controlled Delivery of Ciprofloxacin: Preparation and Evaluation. *Int. J. Biol. Macromol.* **2021**, *176*, 459−467.
(25) Alalaiwe, A.; Carpinone, P.; Alshahrani, S.; Alsulays, B.; Ansari, M.; Anwer, M.; Alshehri, S.; Alshetaili, A. Influence of Chitosan Coating on the Oral Bioavailability of Gold Nanoparticles in Rats. *Saudi Pharm. J.* **2019**, *27*, 171−175.
(26) Eid, H. M.; Elkomy, M. H.; El Menshawe, S. F.; Salem, H. F. Development, Optimization, and in Vitro/in Vivo Characterization of Enhanced Lipid Nanoparticles for Ocular Delivery of Ofloxacin: The Influence of Pegylation and Chitosan Coating. *AAPS PharmSciTech* **2019**, *20*, 1−14.
(27) Takeuchi, I.; Ariyama, M.; Makino, K. Chitosan Coating Effect on Cellular Uptake of PLGA Nanoparticles for Boron Neutron Capture Therapy. *J. Oleo Sci.* **2019**, *68*, No. ess18239.
(28) Bagde, A.; Kouagou, E.; Singh, M. Formulation of Topical Flurbiprofen Solid Lipid Nanoparticle Gel Formulation Using Hot Melt Extrusion Technique. *AAPS PharmSciTech* **2022**, *23*, No. 257.
(29) Rehman, M. U.; Khan, M. A.; Khan, W. S.; Shafique, M.; Khan, M. Fabrication of Niclosamide Loaded Solid Lipid Nanoparticles: In Vitro Characterization and Comparative in Vivo Evaluation. *Artif. Cells, Nanomed., Biotechnol.* **2018**, *46*, 1926−1934.
(30) Al-Adham, I. S. I.; Khalil, E.; Al-Hmoud, N. D.; Kierans, M.; Collier, P. J. Microemulsions Are Membrane-active, Antimicrobial, Self-preserving Systems. *J. Appl. Microbiol.* **2000**, *89*, 32−39.
(31) Jain, S. K.; Chourasia, M. K.; Masuriha, R.; Soni, V.; Jain, A.; Jain, N. K.; Gupta, Y. Solid Lipid Nanoparticles Bearing Flurbiprofen for Transdermal Delivery. *Drug Delivery* **2005**, *12*, 207−215.
(32) Nawaz, A.; Wong, T. W. Microwave as Skin Permeation Enhancer for Transdermal Drug Deliveryery of Chitosan-5-Fluorouracil Nanoparticles. *Carbohydr. Polym.* **2017**, *157*, 906−919.
(33) Agnihotri, S. A.; Jawalkar, S. S.; Aminabhavi, T. M. Controlled Release of Cephalexin through Gellan Gum Beads: Effect of Formulation Parameters on Entrapment Efficiency, Size, and Drug Release. *Eur. J. Pharm. Biopharm.* **2006**, *63*, 249−261.
(34) Yin, C.; Li, X. Anomalous Diffusion of Drug Release from a Slab Matrix: Fractional Diffusion Models. *Int. J. Pharm.* **2011**, *418*, 78−87.
(35) Das, S.; Chaudhury, A. Recent Advances in Lipid Nanoparticle Formulations with Solid Matrix for Oral Drug Deliveryery. *AAPS PharmSciTech* **2011**, *12*, 62−76.
(36) Nazar, M.; Shah, M. U. H.; Yahya, W. Z. N.; Goto, M.; Moniruzzaman, M. Surface Active Ionic Liquid and Tween-80 Blend as an Effective Dispersant for Crude Oil Spill Remediation. *Environ. Technol. Innovation* **2021**, *24*, No. 101868.
(37) Shah, S. N. H.; Asghar, S.; Choudhry, M. A.; Akash, M. S. H.; Rehman, N. ur.; Baksh, S. Formulation and Evaluation of Natural Gum-Based Sustained Release Matrix Tablets of Flurbiprofen Using Response Surface Methodology. *Drug Dev. Ind. Pharm.* **2009**, *35*, 1470−1478.
(38) Danaei, M.; Dehghankhold, M.; Ataei, S.; Hasanzadeh Davarani, F.; Javanmard, R.; Dokhani, A.; Khorasani, S.; Mozafari, M. R. Impact of Particle Size and Polydispersity Index on the Clinical Applications of Lipidic Nanocarrier Systems. *Pharmaceutics* **2018**, *10*, No. 57.
(39) Liu, J.; Hu, W.; Chen, H.; Ni, Q.; Xu, H.; Yang, X. Isotretinoin-Loaded Solid Lipid Nanoparticles with Skin Targeting for Topical Delivery. *Int. J. Pharm.* **2007**, *328*, 191−195.
(40) Yue, Z.-G.; Wei, W.; Lv, P.-P.; Yue, H.; Wang, L.-Y.; Su, Z.-G.; Ma, G.-H. Surface Charge Affects Cellular Uptake and Intracellular Trafficking of Chitosan-Based Nanoparticles. *Biomacromolecules* **2011**, *12*, 2440−2446.
(41) Schmid-Wendtner, M.-H.; Korting, H. C. The PH of the Skin Surface and Its Impact on the Barrier Function. *Skin Pharmacol. Physiol.* **2006**, *19*, 296−302.
(42) Krawczyk, J. Surface Free Energy of the Human Skin and Its Critical Surface Tension of Wetting in the Skin/Surfactant Aqueous Solution/Air System. *Skin Res. Technol.* **2015**, *21*, 214−223.
(43) Podlogar, F.; Rogač, M. B.; Gašperlin, M. The Effect of Internal Structure of Selected Water−Tween 40−Imwitor 308−IPM Microemulsions on Ketoprofene Release. *Int. J. Pharm.* **2005**, *302*, 68−77.
(44) Casariego, A.; Souza, B. W. S.; Vicente, A. A.; Teixeira, J. A.; Cruz, L.; Díaz, R. Chitosan Coating Surface Properties as Affected by Plasticizer, Surfactant and Polymer Concentrations in Relation to the Surface Properties of Tomato and Carrot. *Food Hydrocolloids* **2008**, *22*, 1452−1459.
(45) Fabra, M. J.; Jiménez, A.; Atarés, L.; Talens, P.; Chiralt, A. Effect of Fatty Acids and Beeswax Addition on Properties of Sodium

https://doi.org/10.1021/acsomega.2c08135
ACS Omega 2023, 8, 19302−19310

Caseinate Dispersions and Films. *Biomacromolecules* **2009**, *10*, 1500−1507.
(46) Lee, J. Drug Nano-and Microparticles Processed into Solid Dosage Forms: Physical Properties. *J. Pharm. Sci.* **2003**, *92*, 2057−2068.
(47) Singhvi, G.; Singh, M. In-Vitro Drug Release Characterization Models. *Int. J. Pharm. Stud. Res.* **2011**, *2*, 77−84.
(48) Li, P.; Dai, Y.-N.; Zhang, J.-P.; Wang, A.-Q.; Wei, Q. Chitosan-Alginate Nanoparticles as a Novel Drug Deliveryery System for Nifedipine. *Int. J. Biomed. Sci.* **2008**, *4*, 221−227.
(49) Choi, W. Il.; Lee, J. H.; Kim, J.-Y.; Kim, J.-C.; Kim, Y. H.; Tae, G. Efficient Skin Permeation of Soluble Proteins via Flexible and Functional Nano-Carrier. *J. Controlled Release* **2012**, *157*, 272−278.
(50) Taveira, S. F.; Nomizo, A.; Lopez, R. F. V. Effect of the Iontophoresis of a Chitosan Gel on Doxorubicin Skin Penetration and Cytotoxicity. *J. Controlled Release* **2009**, *134*, 35−40.
(51) Moser, K.; Kriwet, K.; Froehlich, C.; Kalia, Y. N.; Guy, R. H. Supersaturation: Enhancement of Skin Penetration and Permeation of a Lipophilic Drug. *Pharm. Res.* **2001**, *18*, 1006−1011.
(52) Kawadkar, J.; Chauhan, M. K. Intra-Articular Delivery of Genipin Cross-Linked Chitosan Microspheres of Flurbiprofen: Preparation, Characterization, in Vitro and in Vivo Studies. *Eur. J. Pharm. Biopharm.* **2012**, *81*, 563−572.
(53) Nawaz, A.; Wong, T. W. Quantitative Characterization of Chitosan in the Skin by Fourier-transform Infrared Spectroscopic Imaging and Ninhydrin Assay: Application in Transdermal Sciences. *J. Microsc.* **2016**, *263*, 34−42.

https://doi.org/10.1021/acsomega.2c08135
ACS Omega 2023, 8, 19302−19310